

# Novel Notch signaling inhibitor NSI-1 suppresses nuclear translocation of the Notch intracellular domain

TAKAYA SHIRAIISHI<sup>1</sup>, MASAHIRO SAKAITANI<sup>2</sup>, SATOKO OTSUGURO<sup>3</sup>,  
KATSUMI MAENAKA<sup>3</sup>, TOSHIHARU SUZUKI<sup>1</sup> and TADASHI NAKAYA<sup>1</sup>

<sup>1</sup>Laboratory of Neuroscience, Graduate School of Pharmaceutical Sciences, Hokkaido University,  
Sapporo 060-0812; <sup>2</sup>Lilac Pharma Inc., Hokkaido Collaboration Center, Sapporo 001-0021;

<sup>3</sup>Center for Research and Education on Drug Discovery, Hokkaido University, Sapporo 060-0812, Japan

Received March 5, 2019; Accepted July 2, 2019

DOI: 10.3892/ijmm.2019.4280

**Abstract.** The Notch receptor serves a fundamental role in the regulation of cell fate determination through intracellular signal transmission. Mutation of the Notch receptor results in abnormal active signaling, leading to the development of diseases involving abnormal cell growth, including malignant tumors. Therefore, the Notch signaling pathway is a useful pharmacological target for the treatment of cancer. In the present study, a compound screening system was designed to identify inhibitors of the Notch signaling targeting Notch intracellular domain (NICD). A total of 9,600 compounds were analyzed using the Michigan Cancer Foundation-7 (MCF7) human breast adenocarcinoma cell line and the SH-SY5Y human neuroblastoma cell line with the reporter assay system using an artificial protein encoding a partial Notch carboxyl-terminal fragment fused to the Gal4 DNA-binding domain. The molecular mechanism underlying the inhibition of Notch signaling by a hit compound was further validated using biochemical and cell biological approaches. Using the screening system, a potential candidate, Notch signaling inhibitor-1 (NSI-1), was isolated which showed 50% inhibition at 6.1  $\mu$ M in an exogenous Notch signaling system. In addition, NSI-1 suppressed the nuclear translocation of NICD and endogenous gene expression of hairy and enhancer of split-1, indicating that NSI-1 specifically targets Notch. Notably,

NSI-1 suppressed the cell viability of MCF7 cells and another human breast adenocarcinoma cell line, MDA-MB-231 exhibiting constitutive and high Notch signaling activity, whereas no significant effect was observed in the SH-SY5Y cells bearing a lower Notch signaling activity. NSI-1 significantly suppressed the viability of SH-SY5Y cells expressing exogenous human Notch1. These results indicate that NSI-1 is a novel Notch signaling inhibitor and suggest its potential as a useful drug for the treatment of diseases induced by constitutively active Notch signaling.

## Introduction

Notch, a type I transmembrane protein, functions as a critical receptor for cell-cell signal transmission. Notch signaling serves a key role in the regulation of cell fate through lateral inhibition during neurogenesis (1) and is significantly dependent on the proteolytic cleavage of the Notch receptor and its ligands (2). Following its biosynthesis, Notch is cleaved at the S1 site by furin, also known as paired basic amino acid cleaving enzyme, within the Golgi to generate the mature heterodimeric receptor composed of an extracellular amino-terminal fragment and a membrane-tethered carboxyl-terminal fragment (3,4). The Notch extracellular domain then interacts with Delta/Serrate/LAG-2, a ligand expressed in the cell surface of neighboring cells. Consequently, Notch undergoes sequential cleavages at the S2 and S3 sites by ADAM10 and intramembrane  $\gamma$ -secretase complex, respectively, resulting in the release of the Notch intracellular domain (NICD) fragment into the cytoplasm (5). NICD then translocates into the nucleus and activates the transcription of target genes (6). Notch cleavage by the  $\gamma$ -secretase complex, composed of four transmembrane proteins, Aph-1, Nicastrin, Pen-2 and Presenilin (7-11), is the final step in the generation of NICD. Therefore, the dysregulated  $\gamma$ -secretase-mediated cleavage of Notch results in aberrant downstream signaling, which leads to the development of diseases including malignant tumors (12-14). These observations suggest that Notch signaling can be a potent drug target in cancer cells. Efforts aimed at the identification of Notch signaling inhibitors (15-17) have led to the identification of various compounds capable of suppressing Notch signaling. Furthermore, investigations of Notch inhibitors in clinical

---

*Correspondence to:* Dr Tadashi Nakaya, Laboratory of Neuroscience, Graduate School of Pharmaceutical Sciences, Hokkaido University, Kita 12, Nishi 6, Kita-ku, Sapporo 060-0812, Japan  
E-mail: tadashi.nakaya@pharm.hokudai.ac.jp

*Abbreviations:* MCF-7, Michigan Cancer Foundation-7; ADAM, A disintegrin and metalloproteinase; SV40, simian virus 40; VP16, herpes simplex virus protein 16; Gal4 DBD, Gal4 DNA-binding domain; TGN46, trans golgi network 46; MTT, methyl thiazolyl tetrazolium; NSI-1, Notch signaling inhibitor-1; HES1, hairy and enhancer of split-1; DAPI, 4',6-diamidino-2-phenylindole; RLU, relative light units

*Key words:* Notch, cancer, Notch intracellular domain, nuclear translocation, compound screening

trials have demonstrated that the inhibition of Notch signaling promises to be an effective cancer therapy (13,16,17). N-[N-(3,5-difluorophenacetyl)-l-alanyl]-S-phenylglycine t-butyl ester (DAPT) is a well-characterized compound that inhibits  $\gamma$ -secretase by binding to the carboxyl-terminal fragment of presenilin (18), a catalytic component of the  $\gamma$ -secretase complex. As the activity of Notch signaling is dependent on the generation of NICD by  $\gamma$ -secretase,  $\gamma$ -secretase inhibitors, such as DAPT, effectively inhibit Notch signaling in cells. However,  $\gamma$ -secretase targets >100 type I membrane proteins (19), suggesting that inhibiting Notch signaling specifically may be difficult. The present study aimed to identify novel anti-Notch signaling drugs by designing a compound screening system and isolating compounds capable of inhibiting NICD function. Following the screening of 9,600 compounds and performing validation experiments, the compound Notch signaling inhibitor-1 (NSI-1) was isolated, which suppresses Notch signaling by inhibiting the nuclear translocation of NICD. In addition, it was demonstrated that NSI-1 successfully suppressed cell proliferation in Michigan Cancer Foundation-7 (MCF-7) and MDA-MB-231 breast cancer cell lines. Therefore, these findings suggest that NSI-1 may be a useful anticancer drug that targets Notch signaling through a novel mechanism.

## Materials and methods

**Plasmid construction.** The sequences of the constructs utilized in the present study were confirmed using a DNA sequencer (ABI 3130xl genetic analyzer; Thermo Fisher Scientific, Inc.). All of PCR amplifications were performed with Thermal cycler DICE (Takara Bio, Inc., Otsu, Japan) using Ex Taq polymerase (Takara Bio, Inc., Otsu, Japan) otherwise indicated. The Notch $\Delta$ E $\Delta$ Gal4 construct was generated using the following subcloning steps: The signal sequence (ss)-coding cDNA (1-63 bp) and the Notch truncated fragment [ $\Delta$ E $\Delta$ -coding cDNA (5,161-6,609 bp)] of human Notch1 were amplified by PCR (for ss, 96°C, 30 sec, 57°C, 30 sec, 72°C, 15 sec, 22 cycles, for  $\Delta$ E $\Delta$ , 96°C, 30 sec, 57°C, 30 sec, 72°C, 1 min, 22 cycles) using specific primer sets (forward for ss, 5'-TATAGAATTCATGCC GCCGCTCCTGGCGCCCCTG-3'; reverse for ss, 5'-CTC GCCGCACGAGGCGTGCAGAGTGAGACC-3', forward for  $\Delta$ E $\Delta$ , 5'-GGTCTCACTCTGCACGCCTCGTGC GAG-3'; reverse for  $\Delta$ E $\Delta$ , 5'-CTTCTCGAGCAGGGAGTC CACGGGCGA-3') with the hNotch1/pcAMP plasmid (20) as a template. The resulting cDNA fragments were combined by PCR (96°C, 30 sec, 57°C, 30 sec, 72°C, 1 min, 22 cycles; forward, 5'-TATAGAATTCATGCCGCCGCTCCTGGCGCC CCTG-3'; reverse, 5'-CTTCTCGAGCAGGGAGTCCACGGG CGA-3') to obtain the ss- $\Delta$ E $\Delta$  cDNA fragment containing *EcoRI* and *XhoI* digestion sites at the 5' and 3' ends, respectively. A cDNA fragment coding FLAG tag with a methionine accompanying *XhoI* and *ApaI* digestion sites at the 5' and 3' ends, respectively, was synthesized and ligated to the 3' end of the ss- $\Delta$ E $\Delta$  cDNA fragment to obtain ss- $\Delta$ E $\Delta$ -FLAG. This fragment was then digested with *EcoRI* and *ApaI* and subsequently ligated to pcDNA3.1/hygro (V870-20; Thermo Fisher Scientific, Inc.), which was previously digested with *EcoRI* and *ApaI*, to obtain ss- $\Delta$ E $\Delta$ -FLAG/pcDNA3.1hygro. cDNA coding the Gal4 DNA-binding domain (Gal4DBD) was obtained from the pBIND vector (Promega, cat. no. E2440) by digesting

with *XhoI* and *ApaI*. ss- $\Delta$ E $\Delta$ -FLAG/pcDNA3.1hygro was also digested with *XhoI* and *ApaI* and ligated to Gal4DBD to obtain ss- $\Delta$ E $\Delta$ -Gal4DBD/pcDNA3.1hygro. The herpes simplex virus protein 16 (VP16)-coding cDNA containing *XhoI* and *XbaI* digestion sites at the 5' and 3' ends, respectively, was prepared from pACT (Promega, cat. no. C9360) by PCR (96°C, 30 sec, 57°C, 30 sec, 72°C, 15 sec, 25 cycles) with a specific primer set (forward, 5'-ATCTCGACGGCCCCCGCA-3'; reverse, 5'-TCCC GGACCCGGGGAATC-3') and digested with *XhoI* and *XbaI*. ss- $\Delta$ E $\Delta$ -Gal4DBD/pcDNA3.1hygro was also digested with *XhoI* and *XbaI* and ligated to VP16 to obtain ss- $\Delta$ E $\Delta$ -VP16-Gal4DBD/pcDNA3.1hygro, which was then digested with *EcoRI* and *PmeI* to obtain the cDNA fragment ss- $\Delta$ E $\Delta$ -VP16-Gal4DBD. The Piggybac vector (SBI, PB513B-1) was digested with *EcoRI*. Both the ss- $\Delta$ E $\Delta$ -VP16-Gal4DBD fragment and the pre-digested PiggyBac vector were blunted using T4 DNA polymerase and ligated to obtain Notch-ss- $\Delta$ E $\Delta$ -VP16-Gal4DBD/PiggyBac.

The pG5luc/PiggyBac construct was generated using the following subcloning steps: cDNA encoding luciferase was obtained from the pG5luc vector (Promega, cat. no. E2440) by digestion with *NotI* and *BamHI*. The Piggybac vector was digested with *BstXI* and *SpeI*. Subsequently, both the fragments were blunted and ligated to obtain pG5luc/PiggyBac.

The simian virus 40 (SV40) LucGreenPuro/PiggyBac construct was generated using the following subcloning steps: The DNA fragment containing the SV40 promoter was obtained from pcDNA3.1 by digesting with *VspI* and *SmaI*. The PiggyBac vector was digested with *SpeI* and *XbaI* and ligated to SV40 to obtain SV40/PiggyBac. cDNA encoding luciferase was obtained by digestion of pG5luc with *HindIII* and *BamHI*. SV40/PiggyBac was then digested with *EcoRI* and *BamHI*, blunted, and ligated to obtain SV40LucGreenPuro/PiggyBac.

To obtain C99-Gal4/pBIND, C99-coding cDNA was amplified from a plasmid previously described (21) using a specific primer set (forward, 5'-TATAGGATCCCCCA CCATGCTGCCCGG-3'; reverse, 5'-TATAGGTACCGTTCT GCATCTGCTC-3'; 95°C, 10 sec, 57°C, 30 sec, 72°C, 1 min, 22 cycles), digested with *BamHI* and *KpnI*, and cloned into the pBIND vector at the sites.

To obtain Notch1/pcDNA3.1, human Notch1 full-length coding cDNA containing *EcoRI* and *XhoI* sites at the 5' and 3' ends, respectively, was prepared from the hNotch1/pcAMP plasmid using a specific primer set by PCR (forward, 5'-TAT AGAATTCGACGATGCCGCCGCTCCTGGCG-3', reverse, 5'-TATACTCGAGCTATTACTTGAAGGCCTCCGG-3', 95°C, 10 sec, 57°C, 30 sec, 72°C, 3 min, 25 cycles) and cloned into the sites of pcDNA3.1 (Thermo Fisher Scientific, Inc.). Construction of NFLAG-hFE65/pcDNA3.1 was completed as previously described (22).

To obtain NotchICD constructs used in Fig. S1, first NotchICD-VP16-Gal4/pcDNA3.1 was prepared, which included NotchICD full length. Total RNA was isolated from MDA-MB-231 cells, reverse transcribed to obtain 1st cDNA (45°C, 60 min followed by 95°C, 5 min) using the Prime Script 1st strand cDNA Synthesis kit (Takara Bio, Inc.). Following PCR procedures were performed using PrimeSTAR Max DNA polymerase (Takara Bio, Inc.). Notch-ICD for Notch1, Notch2 and Notch3 were amplified by PCR (98°C, 10 sec, 68°C, 2 min, 32 cycles) using primer sets

as follows: Notch1ICD forward, 5'-CCGAATCCCCACCATGGTGCTGTGCCCGCAAG-3' and reverse, 5'-CGCCTCGAGTACTTGAAGGCTCCGGAATG-3'; Notch2ICD forward, 5'-CCGAATCCACCATGGTAATCATGGCAAACG-3' and reverse, 5'-CGCCTCGAGTCACGCATAAACCTGCATG-3'; Notch3ICD forward, 5'-CCGAATCCACCATGGCCCCGGCGCAAGCG-3' and reverse, 5'-CGCCTCGAGTCAGGCCAACACTTGCCTC-3'. Amplified cDNA fragments were digested with *EcoRI* and *XhoI* and cloned into VP16-Gal4/pCDNA3.1. Notch1ICDΔ-VP16-Gal4/pCDNA3.1 was constructed via inverse PCR (98°C, 10 sec, 68°C, 4 min, 12 cycles) using the above-mentioned plasmids as a template and the following primer sets: Notch1ICDΔ forward, 5'-CGCAATGGGCGGTAGGCGTG-3' and reverse, 5'-GAACGGGGAGGGCAGCAGTGG-3'; Notch2ICDΔ forward, 5'-CGCAATGGGCGGTAGGCGTG-3' and reverse, 5'-ATCCATATGGTCTGTGATGTC-3'; Notch3ICDΔ forward, 5'-CGCAATGGGCGGTAGGCGTG-3' and reverse, 5'-GGTGATCTCACGGTTGGCAAAG-3'. The transfection efficacy of plasmid was confirmed by quantitative PCR and immunostain (Figs. S2 and S3).

**Cell culture and plasmid transfection.** Two human breast adenocarcinoma cell lines, MCF-7 (ATCC, cat. no. HTB-22) and MDA-MB-231 (ATCC, cat. no. CRM-HTB-2) and the SH-SY5Y human neuroblastoma cell line (ATCC, cat. no. CRL-2266) were maintained in DMEM (Wako) supplemented with 5% FBS (MP Biomedicals, cat. no. 2916754) at 37°C, 5% CO<sub>2</sub>. All cell lines were purchased from ATCC, guaranteed as Mycoplasma negative. It was also confirmed that they exhibited fine nuclear DAPI staining without additional stains. The plasmids were transfected using Lipofectamine 2000 (Thermo Fisher Scientific, Inc.) following the manufacturer's protocol. To obtain stably transfected MCF7 cell lines, the MCF7 cells were transiently transfected with plasmids and then subjected to drug selection with Geneticin (Wako Pure Chemical Industries, Ltd., Osaka, Japan). A clone was then selected by the abundance of luciferase activity.

**Compound screening.** The 'Core Library' containing 9,600 compounds was provided by the Drug Discovery Initiative at the University of Tokyo. MCF-7 cells stably transfected with Notch-ss-ΔEΔVP16Gal4/PiggyBac and pG5luc/PiggyBac were used for the initial screening. The stable MCF-7 cells (8x10<sup>4</sup>/well) were plated onto a 96-well plate. After 24 h, the medium was replaced with fresh medium containing the compounds (10 μM) and allowed to incubate at 37°C for 24 h. The luciferase activity was then measured using the Steady-Glo luciferase assay system (Promega) and 2300 EnSpire (PerkinElmer, Inc.) according to the manufacturer's protocol. The first candidates that showed >30% inhibitory activity relative to the DMSO control were selected. The hit compounds were further validated with transiently transfected SH-SY5Y cells using the same protocol as that described above. The same procedure was used with the SV40LucGreenPuro/PiggyBac plasmid to exclude false positive compounds.

**Preparation of derivatives.** All commercial reagents were purchased from Wako Pure Chemical Industries, Ltd.. The

synthesized compound was characterized using thin-layer chromatography (TLC), mass spectrometry (MS) and nuclear magnetic resonance (NMR). TLC was performed on a Wakogel FM plate. All microwave syntheses were performed in the Biotage Initiator. <sup>1</sup>H NMR spectra were recorded with JEOL JNM-ECX400P (400 MHz) or JEOL JNM-ECX400 (400 MHz). Chemical shift was expressed as delta values relative to tetramethylsilane (TMS) in units of parts per million (ppm) with TMS as an internal standard. MS was conducted in the LPLC system with Waters SQ Detector 2. All starting materials were synthesized according to previously reported procedures (23). Flash column chromatography was performed using the Biotage Isolera Prime system. Details of synthesis and structures of the derivatives are described in Data S1.

**Calculation of the 50% inhibition rate (IR50) and minimum effective concentration.** Initially, a sigmoidal curve fitting of the values was obtained from the luciferase reporter assay performed in SH-SY5Y cells with 0.01, 0.1, 1, 10 and 20 μM DAPT or NSI-1 (in triplicate) using R software. The inhibition ratio (IR) from maximum to minimum was then calculated using a sigmoid function. The IR50 was defined as the concentration at 50% of the ratio. The minimum effective concentration used in the present study was calculated as follows: First, the maximum IR of DAPT treatment was calculated from the graph, which was ~85% inhibition induced by 10 μM DAPT. The concentration of NSI-1 that showed the same IR (~85%) was then calculated, rounded and used as the minimum effective concentration (15 μM).

**Reverse transcription-quantitative (RT-q)PCR analysis.** Total RNA was isolated from the cells using TRIzol (Thermo Fisher Scientific, Inc.) following the manufacturer's protocol. Total RNA (5 μg) was subjected to RT (45°C, 60 min followed by 95°C, 5 min) using the Prime Script 1st strand cDNA Synthesis kit (Takara Bio, Inc., Otsu, Japan). cDNA was then subjected to qPCR analysis using the Mx3000P qPCR system (Agilent Technologies, Inc.) with THUNDERBIRD SYBR qPCR mix (Toyobo Life Sciences, Osaka, Japan). PCR condition; 95°C, 15 sec followed by 95°C, 10 sec, 60°C, 30 sec, 40 cycles. The primers used were as follows: Luciferase, forward 5'-TCA AAGAGGCGAACTGTGTG-3' and reverse 5'-TTTTCCGTC ATCGTCTTTCC-3', hairy and enhancer of split-1 (HES1), forward 5'-ACGACACCGGATAAACCAAA-3' and reverse 5'-CGGAGGTGCTTCACTGTCAT-3' and GAPDH, forward 5'-AGGGCTGCTTTAACTCTGGT-3' and reverse 5'-CCC CACTTGATTTTGGAGGA-3'. The 2<sup>-ΔΔC<sub>q</sub></sup> method was used for analysis (24).

**Luciferase assay for C99-Gal4.** The SH-SY5Y cells were transfected with C99-Gal4/pBIND, pG5luc and NFLAG-hFE65/pCDNA3.1 using Lipofectamine 2000 following the manufacturer's protocol and the luciferase assay was performed as described above.

**Immunoblotting.** The immunoblotting procedure was performed as previously described (25). Briefly, the cell lysate prepared with RIPA buffer [50 mM Tris, 150 mM NaCl, 1% (w/v) NP-40, 0.1% (w/v) SDS, 1% (w/v) deoxy-

cholate], protein concentration was determined by Lowry method, was separated by SDS-PAGE (30  $\mu\text{g}/\text{lane}$ ) using 6% polyacrylamide gel, transferred onto a nitrocellulose membrane, blocked with 5% skim milk in tris-buffered saline with 0.05% Tween-20 (TBST) for 1 h at room temperature and probed at 4°C for overnight with specific antibodies listed below. Following 3 washes with TBST and incubation with secondary antibodies at room temperature for 1 h, the protein bands were detected with ECL reagents (GE Healthcare Life Sciences) using the LAS4000 mini system (Fujifilm). The antibodies used were as follows: Mouse monoclonal anti-Gal4DBD (1:200, 630403, Clontech Laboratories, Inc.), anti- $\alpha$ -tubulin (1:500, 017-25031 Wako Pure Chemical Industries, Ltd.), rabbit polyclonal anti-NICD (1:1,000, SAB4502019, Sigma-Aldrich; Merck KGaA), goat polyclonal anti-Notch1 (1:200, sc-6014, Santa Cruz Biotechnology, Inc.), Notch Isoform Antibody Sampler kit (3640, Cell Signaling Technology, Inc., 1:1,000 for all three antibodies), mouse IgG HRP Linked F(ab')<sub>2</sub> Fragment (1:5,000, NA9310V, GE Healthcare Life Sciences), rabbit IgG HRP Linked F(ab')<sub>2</sub> Fragment (1:5,000, NA9340V, GE Healthcare Life Sciences) and donkey anti-goat IgG-HRP (1:5,000, sc-2033, Santa Cruz Biotechnology, Inc.). ImageJ software (NIH, Bethesda, MA, USA, version 1.52f) was used to quantify the protein band intensities.

**Immunostaining.** SH-SY5Y cells were fixed with 4% (w/v) paraformaldehyde in PBS for 10 min at room temperature, permeabilized in 0.25% (w/v) Triton X-100 in PBS for 5 min at room temperature, and blocked with 6% (w/v) bovine serum albumin (BSA, 013-25773, Wako Pure Chemical Industries, Ltd.) in PBS for 10 min at room temperature. The cells were then incubated with primary antibodies diluted with 6% BSA in PBS at 4°C overnight. The primary antibodies used were a mouse monoclonal anti-Gal4DBD antibody (1:4,000, 630403, Clontech Laboratories, Inc.) and a rabbit polyclonal anti-*trans* golgi network 46 (TGN46) antibody (1:200, T-7576, Sigma). Following extensive washes with PBS, the cells were incubated with secondary antibodies (diluted with 6% BSA in PBS) and DAPI (3  $\mu\text{g}/\text{ml}$ ) for 1 h at 4°C. The secondary antibodies used were a goat anti-rabbit IgG coupled with Alexa Fluor 546 (1:1,000, A11010, Thermo Fisher Scientific, Inc.) and a donkey anti-mouse IgG coupled with Alexa Fluor 488 (1:1,000, A21202, Thermo Fisher Scientific, Inc.). Images were captured under a fluorescence microscope (BZ-X700; Keyence Corp.). The fluorescence intensities were quantified using ImageJ software (NIH).

**Cytotoxicity assay.** The cells were cultured with 10  $\mu\text{M}$  DAPT, 15  $\mu\text{M}$  NSI-1 or DMSO, and cell viability was analyzed using an MTT assay at 48 and 72 h after the addition of the reagents. Briefly, the medium was replaced with MTT-containing medium (500  $\mu\text{g}/\text{ml}$ ) and incubated at 37°C for 4 h. The formed formazan was then dissolved with DMSO and the absorbance at 570 nm was measured using the 2300 EnSpire reader (PerkinElmer, Inc.).

**Lactate dehydrogenase (LDH) assay.** For the LDH assay, the cells were cultured with 10  $\mu\text{M}$  DAPT, 15- $\mu\text{M}$  NSI-1 or DMSO, and 100  $\mu\text{l}$  medium was collected at 24, 48 and 72 h

after addition of the reagent. LDH activity was then assayed using the Cytotoxicity LDH Assay kit-WST (CK12, Dojindo Molecular Technologies, Inc.). The absorbance at 490 nm (OD490) was determined using the 2300 EnSpire plate reader (PerkinElmer).

**Statistical analysis.** One-way ANOVA with a Tukey post hoc test was performed using a website ([https://astatsa.com/OneWay\\_Anova\\_with\\_TukeyHSD/](https://astatsa.com/OneWay_Anova_with_TukeyHSD/)) for statistical analyses. However, for the results of the LDH assay for cells treated with DMSO, DAPT or NSI-1, the effect of NSI-1 on the production of NICD by DAPT, the effect of Notch1 on the gene expression of *HES1*, and the effect of NSI-1 on Notch family receptors, Student's t-test was used in Excel 16 for Windows.

## Results

**Screening and identification of compounds suppressing the function of NICD.** To establish the compound screening system, an MCF-7 cell line stably expressing Notch $\Delta\text{E}\Delta\text{Gal4}$  and pG5luc/PiggyBac was generated. Notch $\Delta\text{E}\Delta\text{Gal4}$  encodes a human Notch1 truncated fragment containing amino acids 1,721-2,203, including the S3 cleaving site (between amino acids 1,753 and 1,754), with a 21-amino acid Notch1 signal sequence at its amino terminus and a Gal4 DNA-binding domain (Gal4DBD) at its carboxyl terminus (Fig. 1A). A Gal4-targeting DNA sequence is found upstream of the luciferase gene in pG5luc/PiggyBac. Upon cleavage of Notch $\Delta\text{E}\Delta\text{Gal4}$  by  $\gamma$ -secretase, the generated NICD translocates into the nucleus resulting in luciferase activity (Fig. 1B). A reduction of luciferase activity was set to a specific criterion to identify Notch signaling inhibitors. DAPT (26), which lowers luciferase activity by suppressing the generation of NICD-Gal4, was used as a positive control.

A total of 9,600 compounds were screened from the 'Core library' provided by Drug Discovery Initiative of the University of Tokyo, and 80 compound candidates were obtained that showed <70% luciferase activity compared with that in the DMSO control (Fig. 2, left panel). To exclude cell type-dependency, the human neuroblastoma SH-SY5Y cell line was used to re-screen those compounds with the same system. Of the 80 compounds, 26 compounds showed a reduction consistent with that observed in MCF-7 cells. These 26 compounds were further examined using an SV40 promoter-driven luciferase system to exclude compounds that directly affect luciferase expression and/or activity. Finally, one compound was obtained, Candidate 1 (Fig. 2, left panel), which reduced luciferase activity by ~40%, comparable to the activity reduction observed following DAPT treatment and showed no reduction in the false positive assay compared with the DMSO control (data not shown). Subsequently, to identify a critical scaffold structure for Notch signaling inhibition, four analogs of Candidate 1 with different scaffolds were screened. Among these compounds, Candidate 2 was selected as a potential candidate (Fig. 2, middle panel) as it showed the highest inhibition in luciferase activity assay, similar to the activity observed following DAPT treatment (data not shown). Candidate 2 shared an indole structure with Candidate 1. However, the cyclohexane at amine of 5-hydroxyindole was replaced with an isopropyl group. Cytochrome P450 metabo-

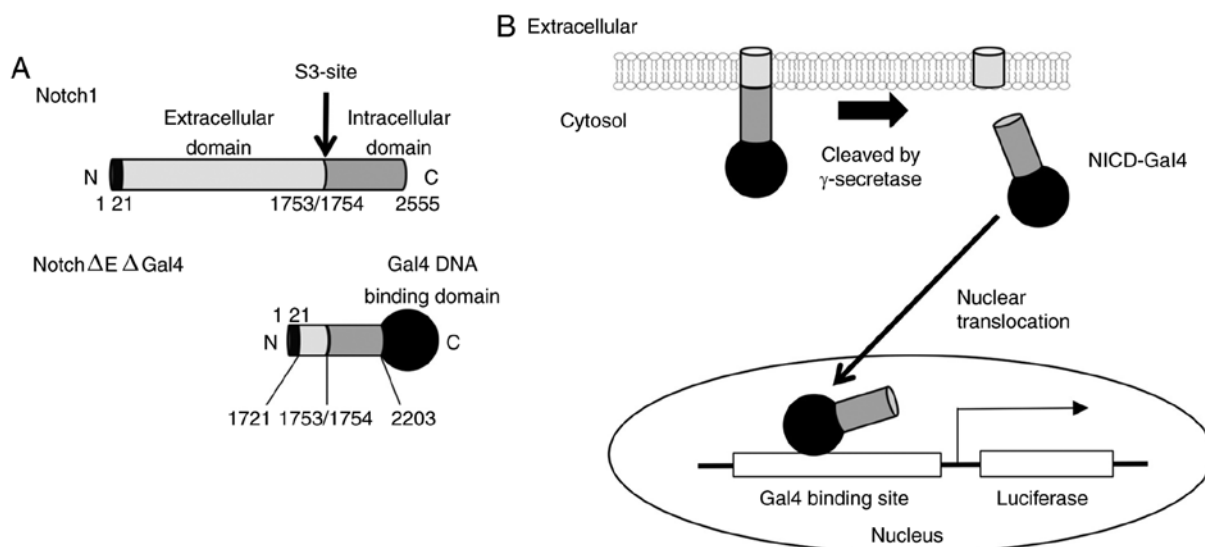


Figure 1. Overview of the screening system used in the identification of Notch signaling inhibitors. (A) Depiction of human Notch1 full-length protein (top) and the Notch $\Delta$ E $\Delta$ Gal4 construct used in the screening system (bottom). Numbers indicate amino acid positions of full-length human Notch1. (B) Depiction of the compound screening system. First,  $\gamma$ -secretase cleaves Notch $\Delta$ E $\Delta$ Gal4 and releases NICD-Gal4, which translocates into the nucleus. NICD-Gal4 then binds to the Gal4-binding sequence upstream of the luciferase gene and induces luciferase transcription. NICD, Notch intracellular domain.

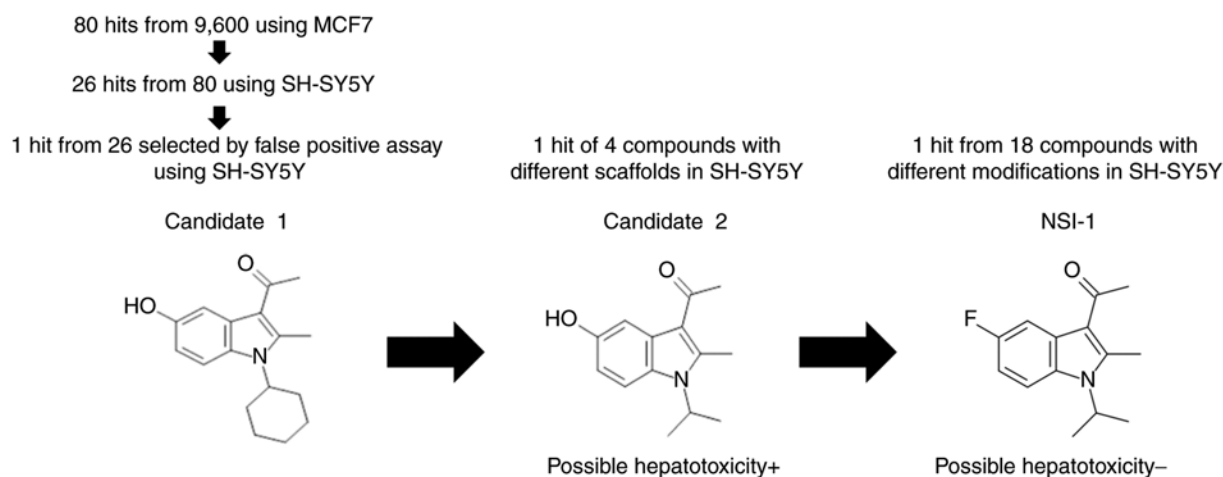


Figure 2. Identification of Notch signaling inhibitor-1 using the screening system. Structures of three compounds obtained through screening are shown. The description above each compound represents the number of hit and total compounds examined and the cell line used. The presence (+) or absence (-) of possible hepatotoxicity is indicated below the compounds. MCF7, Michigan Cancer Foundation-7.

lizes the 5-phenol structure into *p*-imiquinone, which may yield a hepatotoxicity similar to that observed in the conversion of acetaminophen to *N*-acetyl-*p*-benzoquinone imine (27). Therefore, to avoid the 5-phenol structure, 18 derivatives were prepared from Candidate 2 (Data S1) and were used for further screening. Finally, the potential Notch signaling inhibitor 'NSI-1' was identified, in which the hydroxide of 5-phenol had been replaced with fluorine (Fig. 2, right panel).

*NSI-1 is a potential Notch selective inhibitor.* NSI-1 and DAPT treatments resulted in 50% inhibition at  $6.10 \pm 0.16$  and  $1.78 \pm 0.51$   $\mu$ M, respectively, in SH-SY5Y cells using the Notch $\Delta$ E $\Delta$ Gal4-driven system (Fig. 3A). The minimum effective concentrations were determined as 15 and 10  $\mu$ M for NSI-1 and DAPT, respectively, and were used for further analyses. NSI-1 significantly reduced luciferase activity similar to that

observed following DAPT treatment (Fig. 3B;  $24,308 \pm 2,428$  for DMSO,  $7,473 \pm 1,287$  for 10  $\mu$ M DAPT and  $9,833 \pm 1,030$  for 15  $\mu$ M NSI-1,  $n=4$ ,  $P<0.01$  vs. DMSO control). However, no reduction in luciferase activity was observed in SH-SY5Y cells using the SV40-driven system (Fig. 3B,  $17,107 \pm 2,848$  for DMSO,  $17,753 \pm 1,645$  for 10  $\mu$ M DAPT and  $17,390 \pm 3,373$  for 15  $\mu$ M NSI-1,  $n=4$ ). Furthermore, to confirm the effects of NSI-1 on luciferase transcript levels, luciferase mRNA was quantified using RT-qPCR analysis. It was found that NSI-1 and DAPT treatments significantly reduced luciferase transcript levels (Fig. 3C;  $0.19 \pm 0.15$  for 10  $\mu$ M DAPT and  $0.28 \pm 0.11$  for 15  $\mu$ M NSI-1 relative to DMSO control;  $n=3$ ;  $P<0.01$  vs. DMSO control).

To refine the selectivity of NSI-1 for Notch, the effect of NSI-1 on amyloid- $\beta$  precursor protein (APP) processing was analyzed. APP is a type I transmembrane protein that

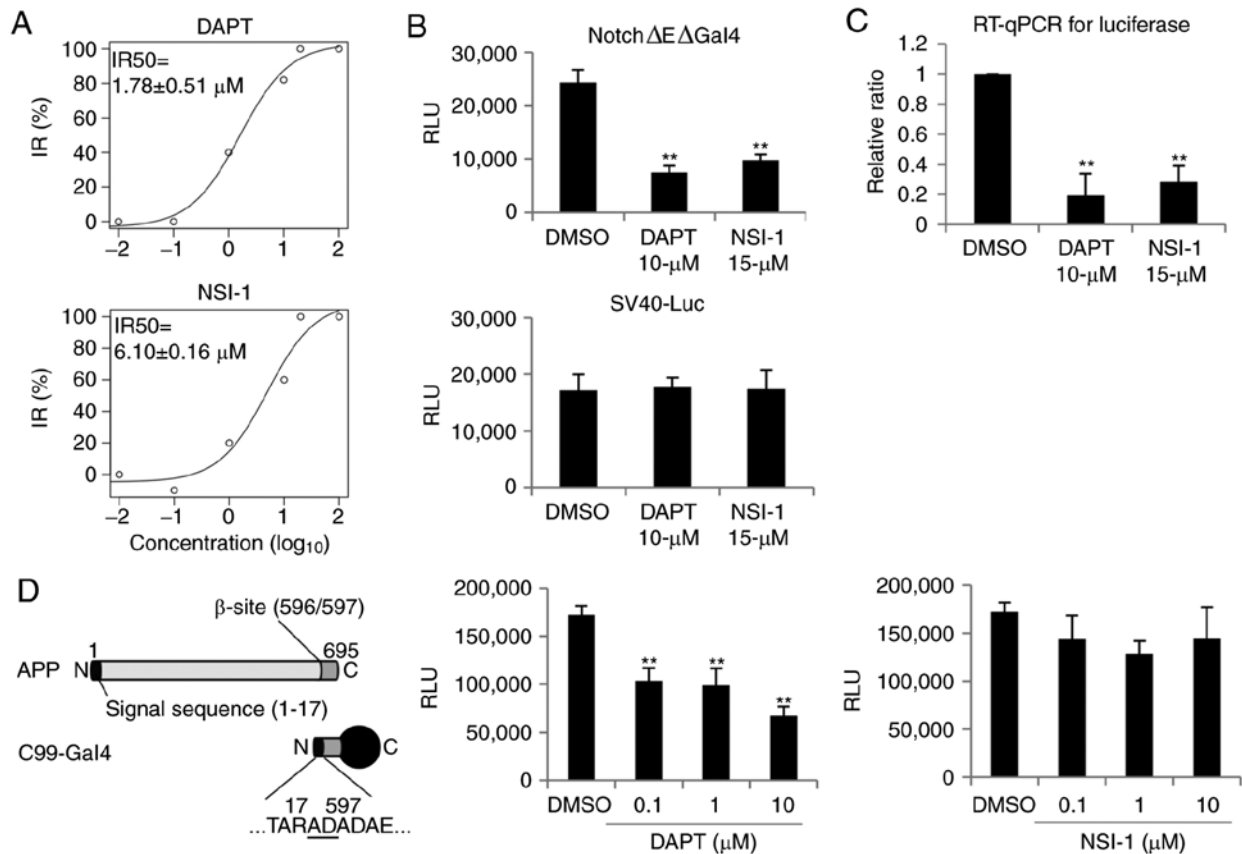


Figure 3. Validation of NSI-1 as a Notch signaling inhibitor. (A) IR<sub>50</sub> of DAPT and NSI-1. The dose-response inhibition curve in luciferase assay systems in SH-SY5Y cells driven by NotchΔEΔGal4 treated with several concentrations of DAPT or NSI-1 was obtained (n=3, mean ± SEM) and the concentration at 50% inhibition was indicated. (B) Validation of NSI-1 activity in luciferase assay systems in SH-SY5Y cells driven by NotchΔEΔGal4 or SV40-Luc. The RLU obtained in a luciferase assay with each treatment are indicated (n=4, mean ± SD; \*\*P<0.01, one-way ANOVA with Tukey post hoc test). (C) Reduction of luciferase gene expression by NSI-1. Expression of luciferase gene assessed by RT-qPCR analysis following indicated treatment in SH-SY5Y cells. The value of the control (DMSO) was set to 1.0 (n=3, mean ± SD; \*\*P<0.01, one-way ANOVA with Tukey post hoc test). (D) Effect of NSI-1 on APP processing. Left, human APP full-length protein (top) and the construct encoding C99-Gal4 (bottom). Numbers indicate amino acid positions of the human APP695 isoform. Right, measurement of luciferase activity in SH-SY5Y cells treated with DMSO (control), DAPT (left) or NSI-1 (right) at indicated concentrations (n=3, mean ± SD; \*\*P<0.01; one-way ANOVA with Tukey post hoc test). NSI-1, Notch signaling inhibitor-1; IR<sub>50</sub>, 50% inhibition rate; RLU, relative light units; DAPT, N-[N-(3,5-difluorophenacetyl)-l-alanyl]-S-phenylglycine t-butyl ester; RT-qPCR, reverse transcription-quantitative PCR; APP, amyloid-β precursor protein.

undergoes a sequential cleavage similar to Notch. Cleavage of APP at the β-site by β-site APP cleaving enzyme 1 releases a large amino-terminal fragment into the extracellular space and leaves a carboxyl-terminal fragment β [CTFβ (C99)] on the membrane. Once γ-secretase cleaves CTFβ at the γ/ε-sites, the intracellular domain is released into the cytoplasm, stabilized by the cytoplasmic protein FE65, and translocated into the nucleus (28). This indicates that CTFβ (C99), which is composed of 99 amino acids of the APP carboxyl-terminal region, is a direct substrate of γ-secretase. The construct C99-Gal4 was constructed encoding C99 bearing the signal sequence of APP at its amino terminus separated by a dipeptide linker Asp + Ala, which was then fused to the amino terminus of Gal4DBD (Fig. 3D). C99-Gal4 and FE65 were expressed in SH-SY5Y cells and the luciferase activity was measured following treatment with DMSO, DAPT or NSI-1. Consistent with a previous report (29), DAPT significantly suppressed the transactivation activity in a dose-dependent manner (Fig. 3D, 172,100 ± 9,699 for DMSO, 103,613 ± 13,409, 98,900 ± 17,761 and 67,580 ± 9,279 for 0.1, 1 and 10 μM DAPT treatment, respectively, n=3, P<0.01 vs. DMSO control). In contrast to DAPT

treatment, treatment with NSI-1 did not result in a significant reduction of activity, even at 10 μM (Fig. 3D, 144,007 ± 24,273, 128,397 ± 13,415 and 144,113 ± 33,005 for 0.1, 1 and 10 μM NSI-1, respectively, n=3, P<0.01 vs. DMSO control), suggesting that NSI-1 selectively acts on Notch.

*NSI-1 suppresses the nuclear translocation of NICD.* To determine the molecular target of NSI-1, the level of NICD generated from the NotchΔEΔGal4 protein in the lysates of cells treated with DMSO, DAPT or NSI-1 was first investigated by immunoblotting with an anti-Gal4DBD antibody. Three specific protein bands were identified (arrowhead and two arrows in top panel of Fig. 4A). An anti-NICD-specific antibody detected two faster migrating protein bands (arrows in middle panel in Fig. 4A), indicating that they represent NICD-Gal4, whereas the slower migrating protein band represents NotchΔEΔGal4 (arrowhead in top panel in Fig. 4A). These results were confirmed by a significant decrease of the two faster migrating bands when treated with 10 μM DAPT (graph in Fig. 4A, 0.33 ± 0.09 for 10 μM DAPT, n=3, P<0.01 vs. DMSO control). By contrast, no significant quantitative

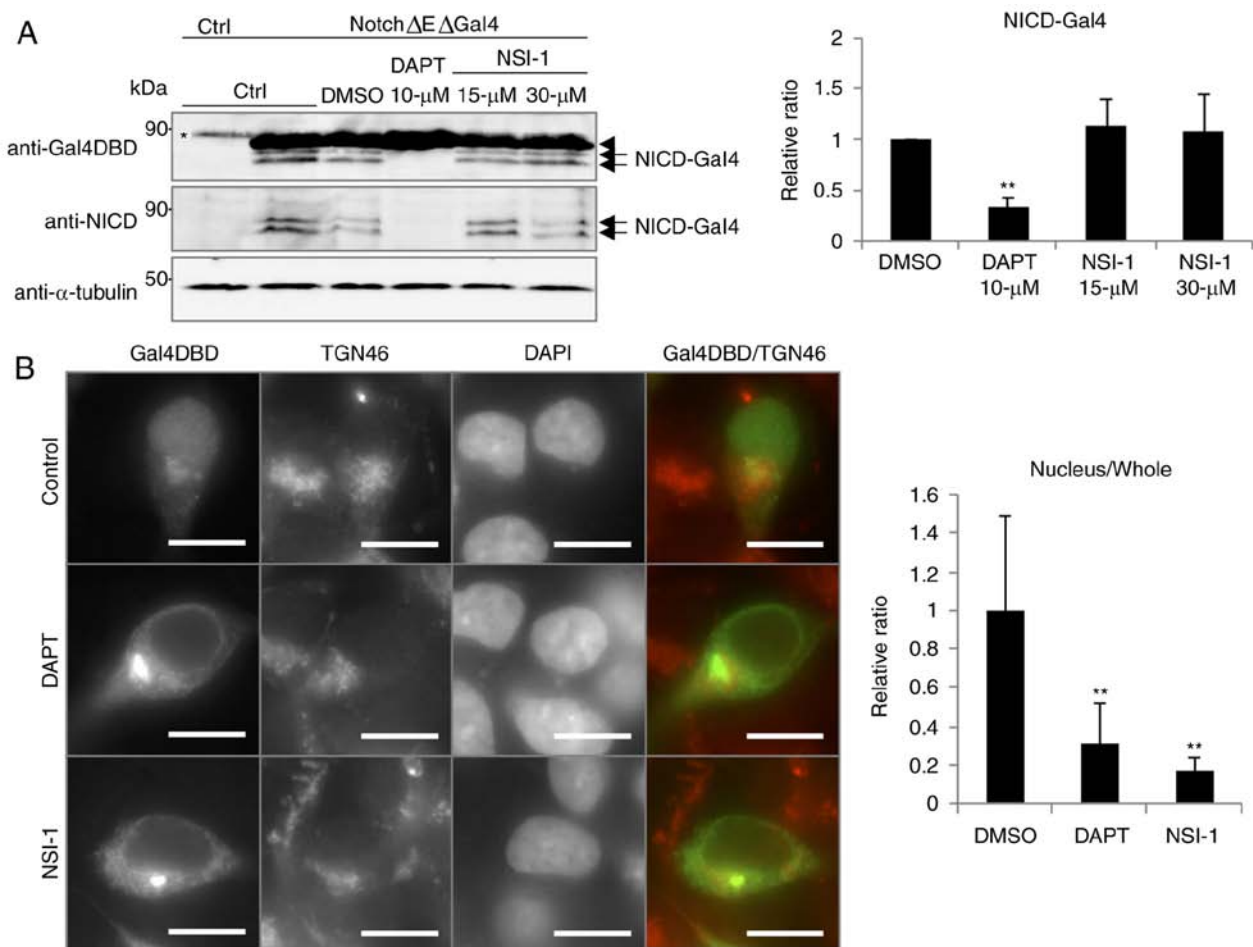


Figure 4. NSI-1 inhibits the nuclear translocation of NICD. (A) Effect of NSI-1 on the processing of Notch $\Delta$ E $\Delta$ Gal4. Immunoblot analysis of NICD-Gal4 in SH-SY5Y cells expressing Notch $\Delta$ E $\Delta$ Gal4 or control (no exogenous protein) following treatment with DMSO, DAPT (10  $\mu$ M), or NSI-1 (15 and 30  $\mu$ M). Arrowhead and arrows indicate Notch $\Delta$ E $\Delta$ Gal4 and NICD-Gal4, respectively. Asterisk indicates a non-specific protein band. The graph shows the relative ratio of NICD-Gal4 protein band intensities to control sample (n=3, mean  $\pm$  SD; \*\*P<0.01, one-way ANOVA with Tukey post hoc test). (B) Localization of Notch $\Delta$ E $\Delta$ Gal4 and NICD-Gal4. Representative images show Notch $\Delta$ E $\Delta$ Gal4-expressing SH-SY5Y cells treated with DMSO control (top panels), 10  $\mu$ M DAPT (middle panels), or 15  $\mu$ M NSI-1 (bottom panels) for 24 h and immunostained with anti-Gal4DBD (left), anti-TGN46 (middle left), and DAPI (middle right). Merged images of cells immunostained with anti-Gal4DBD and anti-TGN46 are shown on the right. Scale bar, 10  $\mu$ m. The graph shows the ratio of intensities in the nucleus to the whole region quantified and normalized to the ratio of DMSO-treated cells (n=10, mean  $\pm$  SD; \*\*P<0.01, one-way ANOVA with Tukey post hoc test). NSI-1, Notch signaling inhibitor-1; NICD, Notch intracellular domain; DAPT, N-[N-(3,5-difluorophenacetyl)-l-alanyl]-S-phenylglycine t-butyl ester; Ctrl, control; Gal4DBD, Gal4 DNA-binding domain; TGN46, trans golgi network 46.

decrease of the two NICD-Gal4 bands was observed with either 15 or 30  $\mu$ M NSI-1 (graph in Fig. 4A,  $1.14 \pm 0.26$  for 15  $\mu$ M and  $1.09 \pm 0.35$  for 30  $\mu$ M, n=3). As NSI-1 significantly suppressed luciferase activity at those concentrations (Fig. 3B), the observations indicate that the NSI-1 does not target the generation of NICD.

Subsequently, the localization of the generated NICD was investigated. Cells expressing Notch $\Delta$ E $\Delta$ Gal4 were treated with DMSO, DAPT or NSI-1, and NICD-Gal4 was detected by immunofluorescence using an anti-Gal4DBD antibody. An anti-TGN46 antibody (Golgi marker) and the nuclear dye DAPI were also used. As NICD-Gal4 contains two nuclear localization signals from Notch full-length protein (6), it was expected that it would localize to the nucleus once  $\gamma$ -secretase released it into the cytoplasm. In control cells, the anti-Gal4DBD signal spread through the nucleus and partially co-localized in a cluster with Golgi marker TGN46 (top panels in Fig. 4B). However, in cells treated with DAPT or NSI-1, the anti-Gal4DBD signal accumulated in the extranuclear region

(middle and lower panels in Fig. 4B). In NSI-1 treated cells, the anti-Gal4DBD signal was partially colocalized with Golgi but distributed through the cytoplasm, suggesting that the cleaved NICD is tethered at those sites. Quantification of the nuclear/entire cell signal intensity ratio showed a significant reduction of nuclear signal in cells treated with DAPT and NSI-1 (graph in Fig. 4B,  $1.0 \pm 0.48$  for DMSO,  $0.31 \pm 0.21$  for 10  $\mu$ M DAPT and  $0.17 \pm 0.07$  for 15  $\mu$ M NSI-1, n=10, P<0.01 vs. DMSO control). Although it was not possible to identify the precise location of NICD-Gal4 in cells treated with NSI-1, taken together with the biochemical analysis, the results show that NSI-1 inhibited the nuclear translocation of NICD and suppressed its function.

*NSI-1 suppresses the viability of cultured cell lines dependent on the expression of Notch1.* The effect of NSI-1 on cell viability was then examined. Treatment of the MCF-7 cells with 15  $\mu$ M NSI-1 significantly reduced cell viability at 72 h (left graph in Fig. 5A). Treatment with 10  $\mu$ M DAPT also significantly reduced the cell viability of MCF-7 cells. Similar results

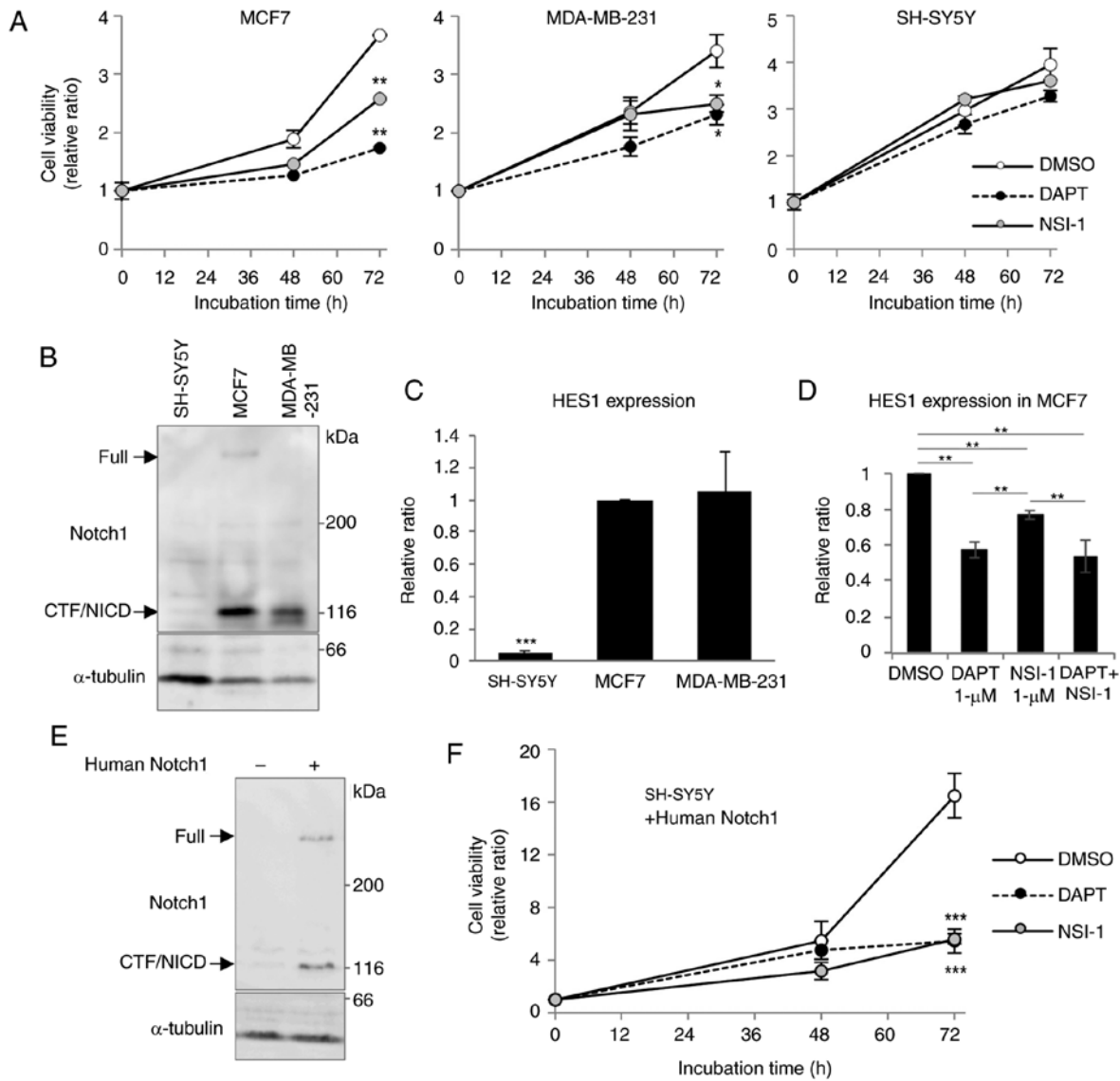


Figure 5. NSI-1 suppresses the viability of cell lines dependent on Notch signaling activity. (A) Effect of NSI-1 on the viability of MCF-7, MDA-MB-231 and SH-SY5Y cells. Viability of MCF-7 (left), MDA-MB-231 (middle) and SH-SY5Y (right) cells treated for 72 h with DMSO, DAPT or NSI-1 (10 or 15  $\mu$ M) was analyzed using an MTT assay. The value at time 0 in each condition was set to 1.0 ( $n=3$ , mean  $\pm$  SD; \*\* $P<0.01$ , \* $P<0.05$ , one-way ANOVA with Tukey post hoc test). (B) Protein expression of Notch1 in MCF-7, MDA-MB-231 and SH-SY5Y cells. Immunoblot analyzing full-length Notch1 (Full), CTF/NICD and  $\alpha$ -tubulin in lysates prepared from MCF-7, MDA-MB-231 and SH-SY5Y cells. Protein standards are indicated on the right. (C) Gene expression of *HES1* in MCF-7, MDA-MB-231 and SH-SY5Y cells. *HES1* gene transcript was quantified by RT-qPCR analysis. The relative ratio to the average value in MCF7 is shown ( $n=3$ , mean  $\pm$  SD; \*\*\* $P<0.005$  vs. MCF7 cells; one-way ANOVA with Tukey post hoc test). (D) Suppression of the gene expression of *HES1* in MCF-7 cells treated with 1  $\mu$ M DAPT, 1  $\mu$ M NSI-1 or 1  $\mu$ M DAPT + 1  $\mu$ M NSI-1. Expression of the *HES1* gene transcript in the treated MCF-7 cells was analyzed by RT-qPCR analysis ( $n=3$ , mean  $\pm$  SD; \*\* $P<0.01$ , one-way ANOVA with Tukey post hoc test). (E) Protein expression of exogenous human Notch1 in SH-SY5Y cells. Cell lysates from vector control (-) and human Notch1-coding plasmid-transfected (+) cells were analyzed. (F) Effect of NSI-1 on the viability of SH-SY5Y cells expressing exogenous human Notch1. NSI-1, Notch signaling inhibitor-1; DAPT, N-[N-(3,5-difluorophenacetyl)-l-alanyl]-S-phenylglycine t-butyl ester; CTF, carboxyl-terminal fragment; NICD, Notch intracellular domain; MCF7, Michigan Cancer Foundation-7;  $n=3$ , mean  $\pm$  SD; \*\*\* $P<0.005$ , one-way ANOVA with Tukey's post hoc test.

were obtained using another human adenocarcinoma line, MDA-MB-231 cells, in which NSI-1 and DAPT significantly suppressed cell viability at 72 h (middle graph in Fig. 5A). Treatment of SH-SY5Y cells did not result in a significant reduction of cell viability (right graph in Fig. 5A). Additionally, their cytotoxicity was analyzed using an LDH assay (Fig. S4). NSI-1 along with DAPT had a minor effect on cytotoxicity compared with that following DMSO treatment, which showed no reverse correlation to the results of the MTT assay shown in Fig. 5A. These results indicate that NSI-1 and DAPT suppress cell proliferation rather than inducing cell death. Considering

the specificity of NSI-1 for Notch signaling, it was considered that endogenous Notch signaling activity may result in different cell viability in MCF-7, MDA-MB-231 and SH-SY5Y cells. Notably, the full-length protein expression of Notch1 was markedly higher in MCF-7 cells than that in SH-SY5Y cells (Fig. 5B). In addition, MCF-7 and MDA-MB-231 cells produced a large amount of Notch1-derived carboxyl-terminal fragment (CTF) and/or NICD, indicating the presence of a constitutively active Notch signaling in those cell lines, which is consistent with a previous report (30). Unlike these cell lines, SH-SY5Y cells showed CTF and/or NICD below the level of

detection (Fig. 5B). To confirm constitutively active Notch signaling in MCF-7 and MDA-MB-231 cells, the expression of endogenous *HES1*, a Notch target gene, was analyzed using RT-qPCR analysis. The expression of *HES1* was significantly higher in the MCF-7 and MDA-MB-231 cells than that in the SH-SY5Y cells (Fig. 5C,  $1.05 \pm 0.25$  for MDA-MB-231 and  $0.05 \pm 0.01$  for SH-SY5Y relative to MCF7,  $P < 0.05$ ,  $n = 3$ ). These results clearly demonstrate that endogenous Notch signaling activity was significantly higher in MCF-7 and MDA-MB-231 cells than that in SH-SY5Y cells. Subsequently, the effect of NSI-1 on Notch target gene expression was investigated, which revealed that NSI-1 significantly suppressed the expression of endogenous *HES1* in MCF-7 cells, similar to DAPT treatment, suggesting that NSI-1 inhibits endogenous Notch signaling (Fig. 5D,  $0.57 \pm 0.04$  for  $1 \mu\text{M}$  DAPT,  $0.77 \pm 0.03$  for  $1 \mu\text{M}$  NSI-1,  $n = 3$ ,  $P < 0.01$  vs. control). There was no additive effect of NSI-1 to DAPT treatment on the expression of *HES1* (Fig. 5D,  $0.54 \pm 0.08$  for  $1 \mu\text{M}$  DAPT +  $1 \mu\text{M}$  NSI-1,  $n = 3$ ,  $P < 0.01$  vs. control). Furthermore, it was confirmed that NSI-1 had no additive effect on the suppressed production of NICD by DAPT treatment (Fig. S5). As DAPT and NSI-1 suppressed Notch signaling but NSI-1 did not facilitate the effect of DAPT on the gene expression of *HES1*, these results suggest that they inhibit the Notch signaling pathway via distinct mechanisms, with NSI-1 suppressing NICD nuclear translocation, and DAPT suppressing NICD production. Finally, the effect of NSI-1 on SH-SY5Y cells expressing exogenous human Notch1 was analyzed. Its expression and cleaved products were confirmed by immunoblotting (Fig. 5E) and it was found that it significantly facilitated the expression of *HES1* (Fig. S6). Treatment of these cells with both  $10 \mu\text{M}$  DAPT and  $15 \mu\text{M}$  NSI-1 significantly suppressed cell viability compared with that in the DMSO control (Fig. 5F,  $5.44 \pm 0.91$  for  $10 \mu\text{M}$  DAPT,  $5.59 \pm 0.39$  for  $15 \mu\text{M}$  NSI-1,  $n = 3$ ,  $P < 0.001$  vs. control), corroborating that NSI-1 specifically targets Notch1 signaling.

## Discussion

The present study identified a novel Notch signaling inhibitor, NSI-1, which inhibited the nuclear translocation of NICD through a mechanism distinct from that used by DAPT, another Notch signaling inhibitor targeting  $\gamma$ -secretase. Notably, NSI-1 had no effect on the cleavage of Notch by  $\gamma$ -secretase. As most of currently developed Notch signaling inhibitors are antibodies specifically targeting Notch and its ligands (16,17), with the exception of  $\gamma$ -secretase inhibitors, NSI-1 is a novel compound that may target Notch signaling through a unique mechanism.

Although how NSI-1 suppresses NICD nuclear translocation remains unclear, the results of the present study clearly showed that NSI-1 had no effect on a general nuclear import mechanism as no significant reduction was observed in C99-Gal4- and SV40-driven systems. Therefore, NSI-1 may act specifically on the localization of NICD. Furthermore, it has been reported that, in addition to nuclear localization signals, post-translational modifications and the interacting proteins are responsible for NICD nuclear localization (31-34). In addition to these specific molecular mechanisms, there is another possibility that NSI-1 induced the aggregation of NICD that suppressed its flexibility. Therefore, additional studies are required to determine which of several possible

molecular mechanisms may be involved in the suppression of the nuclear translocation of NICD by NSI-1. However, NSI-1 appears to be valuable as a suppressor for the Notch signaling pathway.

The desired outcome of Notch signaling inhibition is the induction of cancer cell death or suppression of cancer cell proliferation. Of note, NSI-1 significantly reduced the cell viability of MCF-7 and MDA-MB-231 cells, whereas no effect on SH-SY5Y cells was observed. The present study also showed that DAPT treatment significantly suppressed the cell viability of MCF7 and MDA-MB-231 cells but not of SH-SY5Y cells. Consistent with these results, a previous report demonstrated that Notch signaling was inactive at baseline in SH-SY5Y cells, which was activated by Notch ligands (35). Another report indicated that the level of nuclear NICD was low under a normal condition in SH-SY5Y cells, but was increased when the cells were under oxygen- and glucose-deprived conditions (36). In contrast to these reports and the observations in the present study, reports have indicated that Notch signaling was active in SH-SY5Y cells (37,38). These observations suggest the possibility that Notch signaling in SH-SY5Y cells is susceptible to the experimental conditions, which may be a reason why DAPT and NSI-1 had no effect on SH-SY5Y cells in the present study. As the present study revealed that basic Notch signaling activity was significantly higher in MCF-7 and MDA-MB-231 cells than in SH-SY5Y cells, it was suggested that NSI-1 suppresses the cell viability of MCF-7 and MDA-MB-231 cells through the inhibition of Notch signaling. Notably, NSI-1 significantly reduced the cell viability of the SH-SY5Y cell line expressing exogenous human Notch1, supporting this suggestion. Regardless of the effect of NSI-1 on cell viability, a marginal time-dependent increase of cell viability was observed in the MCF-7 and MDA-MB-231 cells, suggesting that inhibition of the nuclear translocation of NICD may be insufficient for the outcome. Previous studies have shown that targeting Notch signaling with a combination of DAPT and other drugs resulted in a superior anticancer effect (14,39,40). Therefore, a combination of NSI-1 with other drugs may potentially maximize the anticancer effect of NSI-1. Considering anticancer treatments appear to be more effective when Notch signaling is inhibited in cancer and cancer stem cells (41), further studies should investigate the effect of NSI-1 on cancer stem cells.

The present study preliminarily analyzed the effect of NSI-1 on two other Notch family receptors, Notch2 and Notch3, which are expressed in the SH-SY5Y cell line (Fig. S7) (35). Using Notch-ICD-Gal4 constructs, it was found that NSI-1 suppressed the activity of all of those constructs (Fig. S1), indicating that NSI-1 targets not only Notch1 but also Notch2 and Notch3. As Notch family proteins share their protein domains and functions (42), these results suggest that NSI-1 may suppress the nuclear translocation of NICD via a molecular mechanism through common domains of Notch family receptors.

It is important to have a variety of clinical strategies targeting a single critical pathway, such as the Notch signaling pathway. Although further investigations are required to identify its molecular target and to evaluate its advantage for clinical use, the present study suggests NSI-1 is eligible as a seed compound for further development of a novel and unique Notch signaling inhibitor.

## Acknowledgements

The authors would like to thank Mr. Kazuma Tamba (Hokkaido University) and Ms. Madoka Kaneko (Hokkaido University) for providing technical assistance with plasmid preparation and compound library screening. The hNotch1/pcAMP plasmid was kindly provided by Professor Spyros Artavanis-Tsakonas (Artavanis-Tsakonas Laboratory, Department of Cell Biology Harvard Medical School). This study was partially supported by the Platform Project for Supporting in Drug Discovery and Life Science Research (Platform for Drug Discovery, Informatics and Structural Life Science) from the Ministry of Education, Culture, Sports, Science and Technology, and the Japan Agency for Medical Research and Development (AMED). This support comprised research and education on drug discovery for compound library screening.

## Funding

This study was supported in part by a Grants-in-Aid for Scientific Research (grant. no. 16K14690) to TSu from the Ministry of Education, Culture, Sports, Science and Technology, Japan.

## Availability of data and materials

All data generated or analyzed during this study are included in this published article and in the supplementary files.

## Authors' contributions

TSh designed the study, performed all the experiments and wrote the manuscript. MS prepared all derivative compounds and conducted screening experiments with SO and KM. TN and TSu designed and conducted screening and biochemical experiments and wrote the manuscript. All authors have read and approved the final manuscript.

## Ethics approval and consent to participate

Not applicable.

## Patient consent for publication

Not applicable.

## Competing interests

The authors declare that they have no competing interests.

## References

- Cabrera CV: Lateral inhibition and cell fate during neurogenesis in *Drosophila*: The interactions between scute, Notch and Delta. *Development* 110: 733-742, 1990.
- Schroeter EH, Kisslinger JA and Kopan R: Notch-1 signalling requires ligand-induced proteolytic release of intracellular domain. *Nature* 393: 382-386, 1998.
- Logeat F, Bessia C, Brou C, LeBail O, Jarriault S, Seidah NG and Israël A: The Notch1 receptor is cleaved constitutively by a furin-like convertase. *Proc Natl Acad Sci USA* 95: 8108-8112, 1998.
- Blaumueller CM, Qi H, Zagouras P and Artavanis-Tsakonas S: Intracellular cleavage of Notch leads to a heterodimeric receptor on the plasma membrane. *Cell* 90: 281-291, 1997.
- Groot AJ, Habets R, Yahyanejad S, Hodin CM, Reiss K, Saftig P, Theys J and Vooijs M: Regulated proteolysis of NOTCH2 and NOTCH3 receptors by ADAM10 and presenilins. *Mol Cell Biol* 34: 2822-2832, 2014.
- Andersson ER, Sandberg R and Lendahl U: Notch signaling: Simplicity in design, versatility in function. *Development* 138: 3593-3612, 2011.
- Francis R, McGrath G, Zhang J, Ruddy DA, Sym M, Apfeld J, Nicoll M, Maxwell M, Hai B, Ellis MC, *et al*: Aph-1 and pen-2 are required for Notch pathway signaling, gamma-secretase cleavage of betaAPP, and presenilin protein accumulation. *Dev Cell* 3: 85-97, 2002.
- Edbauer D, Winkler E, Regula JT, Pesold B, Steiner H and Haass C: Reconstitution of gamma-secretase activity. *Nat Cell Biol* 5: 486-488, 2003.
- Kimberly WT, LaVoie MJ, Ostaszewski BL, Ye W, Wolfe MS and Selkoe DJ: Gamma-secretase is a membrane protein complex comprised of presenilin, nicastrin, Aph-1, and Pen-2. *Proc Natl Acad Sci USA* 100: 6382-6387, 2003.
- Takasugi N, Tomita T, Hayashi I, Tsuruoka M, Niimura M, Takahashi Y, Thinakaran G and Iwatsubo T: The role of presenilin cofactors in the gamma-secretase complex. *Nature* 422: 438-441, 2003.
- Hayashi I, Urano Y, Fukuda R, Isoo N, Kodama T, Hamakubo T, Tomita T and Iwatsubo T: Selective reconstitution and recovery of functional gamma-secretase complex on budded baculovirus particles. *J Biol Chem* 279: 38040-38046, 2004.
- Mao L: NOTCH mutations: Multiple faces in human malignancies. *Cancer Prev Res (Phila)* 8: 259-261, 2015.
- Pannuti A, Foreman K, Rizzo P, Osipo C, Golde T, Osborne B and Miele L: Targeting Notch to target cancer stem cells. *Clin Cancer Res* 16: 3141-3152, 2010.
- Zhao ZL, Zhang L, Huang CF, Ma SR, Bu LL, Liu JF, Yu GT, Liu B, Gutkind JS, Kulkarni AB, *et al*: NOTCH1 inhibition enhances the efficacy of conventional chemotherapeutic agents by targeting head neck cancer stem cell. *Sci Rep* 6: 24704, 2016.
- Yahyanejad S, Theys J and Vooijs M: Targeting Notch to overcome radiation resistance. *Oncotarget* 7: 7610-7628, 2016.
- Yuan X, Wu H, Xu H, Xiong H, Chu Q, Yu S, Wu GS and Wu K: Notch signaling: An emerging therapeutic target for cancer treatment. *Cancer Lett* 369: 20-27, 2015.
- Andersson ER and Lendahl U: Therapeutic modulation of Notch signalling-are we there yet? *Nat Rev Drug Discov* 13: 357-378, 2014.
- Morohashi Y, Kan T, Tominari Y, Fuwa H, Okamura Y, Watanabe N, Sato C, Natsugari H, Fukuyama T, Iwatsubo T and Tomita T: C-terminal fragment of presenilin is the molecular target of a dipeptidic gamma-secretase-specific inhibitor DAPT (N-[N-(3,5-difluorophenacetyl)-L-alanyl]-S-phenylglycine t-butyl ester). *J Biol Chem* 281: 14670-14676, 2006.
- Haapasalo A and Kovacs DM: The many substrates of presenilin/γ-secretase. *J Alzheimers Dis* 25: 3-28, 2011.
- Mishra-Gorur K, Rand MD, Perez-Villamil B and Artavanis-Tsakonas S: Down-regulation of Delta by proteolytic processing. *J Cell Biol* 159: 313-324, 2002.
- Araki Y, Tomita S, Yamaguchi H, Miyagi N, Sumioka A, Kirino Y and Suzuki T: Novel cadherin-related membrane proteins, Alcadeins, enhance the X11-like protein-mediated stabilization of amyloid beta-protein precursor metabolism. *J Biol Chem* 278: 49448-49458, 2003.
- Ando K, Iijima KI, Elliott JI, Kirino Y and Suzuki T: Phosphorylation-dependent regulation of the interaction of amyloid precursor protein with Fe65 affects the production of beta-amyloid. *J Biol Chem* 276: 40353-40361, 2001.
- Okauchi T, Itonaga M, Minami T, Owa T, Kitoh K and Yoshino H: A general method for acylation of indoles at the 3-position with acyl chlorides in the presence of dialkylaluminum chloride. *Org Lett* 2: 1485-1487, 2000.
- Livak KJ and Schmittgen TD: Analysis of relative gene expression data using real-time quantitative PCR and the 2<sup>-ΔΔC<sub>T</sub></sup> method. *Methods* 25: 402-408, 2001.
- Nakaya T, Kawai T and Suzuki T: Regulation of FE65 nuclear translocation and function by amyloid beta-protein precursor in osmotically stressed cells. *J Biol Chem* 283: 19119-19131, 2008.
- Dovey HF, John V, Anderson JP, Chen LZ, de Saint Andrieu P, Fang LY, Freedman SB, Folmer B, Goldbach E, Holsztynska EJ, *et al*: Functional gamma-secretase inhibitors reduce beta-amyloid peptide levels in brain. *J Neurochem* 76: 173-181, 2001.

27. Albano E, Rundgren M, Harvison PJ, Nelson SD and Moldéus P: Mechanisms of N-acetyl-p-benzoquinone imine cytotoxicity. *Mol Pharmacol* 28: 306-311, 1985.
28. Kimberly WT, Zheng JB, Guénette SY and Selkoe DJ: The intracellular domain of the beta-amyloid precursor protein is stabilized by Fe65 and translocates to the nucleus in a notch-like manner. *J Biol Chem* 276: 40288-40292, 2001.
29. Cao X and Südhof TC: Dissection of amyloid-beta precursor protein-dependent transcriptional transactivation. *J Biol Chem* 279: 24601-24611, 2004.
30. D'Angelo RC, Ouzounova M, Davis A, Choi D, Tchuenkam SM, Kim G, Luther T, Quraishi AA, Senbabaoglu Y, Conley SJ, *et al*: Notch reporter activity in breast cancer cell lines identifies a subset of cells with stem cell activity. *Mol Cancer Ther* 14: 779-787, 2015.
31. Gupta-Rossi N, Le Bail O, Gonen H, Brou C, Logeat F, Six E, Ciechanover A and Israël A: Functional interaction between SEL-10, an F-box protein, and the nuclear form of activated Notch1 receptor. *J Biol Chem* 276: 34371-34378, 2001.
32. Oberg C, Li J, Pauley A, Wolf E, Gurney M and Lendahl U: The Notch intracellular domain is ubiquitinated and negatively regulated by the mammalian Sel-10 homolog. *J Biol Chem* 276: 35847-35853, 2001.
33. Wu G, Lyapina S, Das I, Li J, Gurney M, Pauley A, Chui I, Deshaies RJ and Kitajewski J: SEL-10 is an inhibitor of notch signaling that targets notch for ubiquitin-mediated protein degradation. *Mol Cell Biol* 21: 7403-7415, 2001.
34. Fryer CJ, White JB and Jones KA: Mastermind recruits CycC:CDK8 to phosphorylate the Notch ICD and coordinate activation with turnover. *Mol Cell* 16: 509-520, 2004.
35. Zage PE, Nolo R, Fang W, Stewart J, Garcia-Manero G and Zweidler-McKay PA: Notch pathway activation induces neuroblastoma tumor cell growth arrest. *Pediatr Blood Cancer* 58: 682-689, 2012.
36. Cheng YL, Choi Y, Seow WL, Manzanero S, Sobey CG, Jo DG and Arumugam TV: Evidence that neuronal Notch-1 promotes JNK/c-Jun activation and cell death following ischemic stress. *Brain Res* 1586: 193-202, 2014.
37. Cama A, Verginelli F, Lotti LV, Napolitano F, Morgano A, D'Orazio A, Vacca M, Perconti S, Pepe F, Romani F, *et al*: Integrative genetic, epigenetic and pathological analysis of paraganglioma reveals complex dysregulation of NOTCH signaling. *Acta Neuropathol* 126: 575-594, 2013.
38. Ferrari-Toninelli G, Bonini SA, Uberti D, Buizza L, Bettinsoli P, Poliani PL, Facchetti F and Memo M: Targeting Notch pathway induces growth inhibition and differentiation of neuroblastoma cells. *Neuro Oncol* 12: 1231-1243, 2010.
39. Wang M, Ma X, Wang J, Wang L and Wang Y: Pretreatment with the  $\gamma$ -secretase inhibitor DAPT sensitizes drug-resistant ovarian cancer cells to cisplatin by downregulation of Notch signaling. *Int J Oncol* 44: 1401-1409, 2014.
40. Shah MM, Zerlin M, Li BY, Herzog TJ, Kitajewski JK and Wright JD: The role of Notch and gamma-secretase inhibition in an ovarian cancer model. *Anticancer Res* 33: 801-808, 2013.
41. Qiu H, Fang X, Luo Q and Ouyang G: Cancer stem cells: A potential target for cancer therapy. *Cell Mol Life Sci* 72: 3411-3424, 2015.
42. Crabtree JS, Singleton CS and Miele L: Notch signaling in neuroendocrine tumors. *Front Oncol* 6: 94, 2016.